### Title
Agarose-Based Hydrogels as Suitable Bioprinting Materials for Tissue Engineering




### Journal
ACS Biomaterials Science & Engineering, 4(10)

### ISSN
2373-9878



### Authors
López-Marcial, Gabriel R
Zeng, Anne Y
Osuna, Carlos
et al.



### Publication Date
2018-10-08

### DOI
10.1021/acsbiomaterials.8b00903

Peer reviewed

# Agarose-based hydrogels as suitable bioprinting materials

Gabriel R. López-Marcial[1], Anne Y. Zeng[1], Carlos Osuna[2], Joseph Dennis[3]
Jeannette M. García*[3], Grace D. O'Connell*[1,4]

[1]Department of Mechanical Engineering
University of California, Berkeley

[2]Department of Mechanical Engineering
University of California, San Diego

[3]Department of Chemistry and Materials
IBM Almaden Research Center, San Jose

[4]Department of Orthopaedic Surgery
University of California, San Francisco

Submitted to: ACS Biomaterials Science & Engineering

*Corresponding Authors:
Grace D. O'Connell, PhD.
5122 Etcheverry Hall, #1740
Berkeley, CA 94720
g.oconnell@berkeley.edu

Jeannette M. García
650 Harry Road
San Jose, CA 95120
jmgarcia@us.ibm.com

## Abstract

Hydrogels are useful materials as scaffolds for tissue engineering applications. The solid content used for hydrogels require a balance between scaffold stiffness and nanoporosity, which impacts nutrient diffusion into cell-laden scaffolds. Using hydrogels with additive manufacturing techniques has been a challenge, due to inconsistencies in print fidelity. In this study, agarose-based hydrogels commonly used for cartilage tissue engineering were compared to Pluronic, a hydrogel with established printing capabilities. Moreover, new material mixtures were developed for bioprinting by combining alginate and agarose. We compared mechanical and rheological properties, including yield stress, storage modulus, and shear thinning, to determine parameters that may predict better extrusion-based printability and to assess their potential as a bioink for cell-based tissue engineering. We found that all gels demonstrated shear-thinning behavior, yet recovered immediately upon the absence of a shear stress. Print fidelity of agarose-based gels improved with the addition of alginate, which did not significantly alter yield strength ($p > 0.1$). Alginate-agarose composites prepared with 5% w/v (3:2 agarose to alginate ratio) demonstrated high print fidelity with excellent cell viability that was maintained over a 28-day culture period (>~70% cell survival at day 28). Therefore, agarose-alginate mixtures showed the greatest potential as an effective bioink for additive manufacturing of biological materials for cartilage tissue engineering.



## Keywords

Additive manufacturing, Bioprinting, hydrogels, 3D printing, bioinks, agarose, alginate

## Introduction

Osteoarthritis of articular cartilage leads to chronic pain and reduced joint mobility[1]. The gold-standard treatment strategy for osteoarthritis is total-joint arthroplasty, where the native cartilage and some of the underlying boney tissue are removed and replaced with metal and polymer components. While successful in reducing joint pain, the mismatch in material stiffness between native tissues (0.5-1.0 MPa for cartilage[2, 3]) and implanted materials (0.9 GPa for ultra-high molecular weight polyethylene[4]) causes long-term problems, including increased degradation of the surrounding healthy tissue[5]. Alternatively, tissue-engineering strategies aim to recapitulate the function of healthy cartilage in the laboratory to develop implantable biomaterials for cartilage repair and replacement.

Hydrogels have become common scaffolds for cartilage tissue engineering, because of their ability to promote production of extra cellular matrix components in three-dimensional (3D) culture. Popular hydrogels for matrix production include sodium alginate and agarose. Agarose has been particularly successful in cultivating engineered cartilage constructs with biochemical and mechanical properties comparable to native values within eight weeks of culture[6]. Hydrogel selection is largely based on biocompatibility, nanoporosity, support for matrix deposition, and material behavior under specific temperature ranges or loading conditions (*e.g.*, static *vs*. dynamic loading)[7].

Casting is the preferred fabrication method for thermoset hydrogels, with individual constructs being created with diameters that are typically less than 10 mm[8-11]. Implanting standard casted constructs will require surface shaping to match the patient's native curvature. However, matrix deposition does not occur evenly throughout the construct, with the construct periphery receiving more nutrients, resulting in greater matrix deposition. Therefore, resurfacing

an engineered construct during implantation will weakening the implanted material, altering stress distributions between engineered and native tissues, which may affect long-term durability. Recent studies have shown that clinical images (*i.e.*, magnetic resonance images or computed tomography) can be used to develop molds for larger engineered cartilage surfaces with subject-specific topography[2, 15]. However, cultivating larger constructs is difficult, due to the increase in nutrient path-length between nutrients surrounding the construct and cells at the center of the construct, hindering matrix production and affecting long-term cell viability[12, 1314].

Extrusion-based 3D printing represents an attractive alternative to casting because of the increased versatility in construct design and ability to incorporate macropores throughout the scaffold design[16, 17]. However, 3D printing of hydrogels with high shape fidelity has been difficult due to issues during extrusion and material spreading after being dispensed from the nozzle. Useful materials for extrusion-based printing must demonstrate shear thinning behavior (*i.e.,* non-Newtonian behavior), where viscoelastic properties are shear-rate dependent. That is, these materials must stop flowing once deposited onto the print platform to minimize spreading and maintain shape fidelity.

Recent work by Mouser *et al.* demonstrated that yield strength was an important material property for determining printability, where materials with higher yield strength had better shape fidelity. Thermoset hydrogels are ideal for this purpose, as material properties are tunable based on the concentration of solids in the mixture. Previous studies have also printed hydrogels into a cooling cryogenic liquid (cryoprinting) or into an ion bath to induce crosslinking and improve print fidelity. However, increasing the solid composition and crosslinking affects nanoporosity, which will alter nutrient diffusion and tissue growth. Furthermore, cryoprinting may negatively impact long-term cell viability, if temperature gradients are not carefully controlled throughout

the construct. Therefore, there is a need to develop bioinks that are able to maintain high shape fidelity with extrusion-based printing, without compromising their ability to support *de novo* matrix growth.

The objective of this study was to identify a suitable non-crosslinked hydrogel for bioprinting. Specifically, we investigated mechanical properties of various concentrations and combinations of biocompatible polymers, including agarose (Type VII) and sodium alginate, which were compared to Pluronic F-127, a gel with known printing capabilities (Figure 1). Agarose and sodium alginate have been used extensively for cartilage engineering, because of their ability to promote cell proliferation and matrix production[22-28]. Pluronic was used as a control material for 3D printing; however, it is not considered an ideal bioink for scaffold formation, due to issues with long-term cell viability and stability in aqueous solutions[8, 10, 30-32]. Printable gels were then tested to confirm biocompatibility with cartilage chondrocytes for tissue engineering applications.

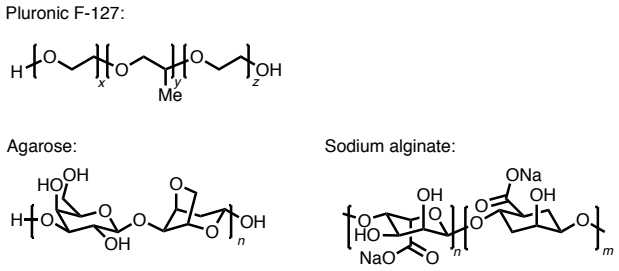


**Figure 1.** Molecular structure of evaluated materials (Pluronic, agarose, and sodium alginate).

## Materials and Methods

*Hydrogel Preparation*

Agarose hydrogels were prepared by mixing agarose in 0.15 M phosphate buffered saline (PBS) for final concentrations of 2%, 3%, or 4% weight by volume (w/v; Type VII powder, Sigma Aldrich, St. Louis, MO). Alginate-agarose hydrogels were prepared by mixing a 3:2 ratio

of agarose and sodium alginate in 0.15 M PBS (total solid content = 3.75% or 5% w/v). All agarose-based hydrogels were mixed and sterilized in a bench-top autoclave (120 °C for 25 minutes). Pluronic® F-127 hydrogels were prepared at a final concentration of 30% w/v in 0.15 M PBS and mixed in an ice bath until a homogeneous clear liquid formed. All solutions gelled within 10 minutes at room temperature.

*Rheology and Mechanical Testing*

Four experiments were performed to evaluate temperature-dependent and strain rate-dependent mechanical properties (Anton Paar MCR302 rheometer, Ashland, VA). Samples (~0.35 g; n = 5 per group) were loaded onto the Peltier plate and a steel plate was lowered to compress the gel sample (conical plate diameter = 25 mm; trimming gap = 64 μm; final gap = 54 μm). Agarose-based gels were re-melted by increasing the temperature of the Peltier plate to 65 °C, then allowed to gel at room temperature before each test.

In the first experiment, the temperature of the Peltier plate was increased at a rate of 5 °C/min under a constant oscillatory stress (1 Pa at 1 Hz). A smoothing function was used to eliminate random peaks in measurements (average of every 5 points). Storage modulus, loss modulus, and phase angle were recorded.

In the second experiment, shear rate was increased from 0.01 to 10.00 $s^{-1}$ and viscosity was measured (temperature = 37 °C). Shear thinning gels were defined as those that followed a power law relationship ($y = \alpha e^{\beta}$); therefore, exhibiting a linear decrease in viscosity with temperature when plotted on logarithmic scale. The parameters α and β were used to calculate shear rate at the extruder wall using a power law relationship for non-Newtonian fluids (Equation 1).[33] In Equation 1, $R$ and $L$ are the radius and length of the extruder needle, respectively, $\gamma_w$ is

the shear rate at the extruder wall, and $\Delta P$ is the pressure difference between the extruder and the atmosphere.

$$\gamma_w = \left(\frac{R\Delta P}{2\alpha L}\right)^{\frac{1}{\beta+1}} \quad (1)$$

The third experiment consisted of applying the calculated shear rate at the extruder wall ($\gamma_w$) for 1000 s at 37°C. The shear yield point was defined as the maximum shear stress measured in that range. The fourth and final experiment consisted of three steps: first, a constant oscillation was applied at 1 Hz for 100 s. Then, the calculated shear rate at the extruder wall was applied for 800 s to induce yield, followed by a constant oscillation (1 Hz, 30 minutes, at 37 °C). Storage (G') and loss (G") moduli were measured during oscillations. The time value where storage modulus was greater than loss modulus during the second oscillation step was defined as the recovery time of the 3D hydrogel network after yielding.

Compressive modulus of agarose-based gel mixtures was determined under unconfined compression testing. Gels were cast into slabs between two glass slides separated with a rubber border (thickness = 2.27 mm). A 6 mm biopsy punch was used to create cylindrical samples from the slab. A monotonic ramp test to 90% strain at a rate of 0.3 %/s was applied to calculate yield strength (n = 10 samples per group; Instron A620-325, Norwood, MA), which was defined as the stress at the end of the linear portion of the stress-strain curve.

*Acellular and Cell-Based Printing*

To evaluate print fidelity, a commercially available 3D printer was used to print simple line and honeycomb structures (BioBots, Philadelphia, PA). Two-dimensional geometries were created using computer-aided design (CAD; AutoCad 2016, Autodesk, San Francisco, CA), converted to 3D stereolithography files (STL, 360 Fusion by Autodesk), which was then converted into g-code to be interpreted by the 3D printer (Repetier software, Willich, Germany).

Hydrogels were loaded into a 10 mL syringe and placed into a heated canister to maintain 37 °C during printing. Gels were extruded through a 30-gauge needle by applying 65–75 psi of pressure with an air compressor. Printed constructs were photographed next to a ruler for scale.

To quantify shape fidelity, a custom algorithm was developed that overlaid the CAD model with pictures of the printed construct and output the amount of (a) overlap between pixels from the printed gel and the CAD model, (b) gel pixels outside of the model area, and (c) model pixels not covered by the gel ($n > 8$; MATLAB, Mathworks, Natick, MA). A printing parameter, p, was defined as the percentage of correctly placed (overlapping) pixels minus the percentage of incorrectly placed (overhanging plus uncovered model) pixels ($p = (a - b - c)*100$; Figure 2).

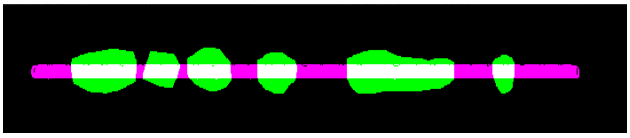

**Figure 2.** Example output of overlaid images from MATLAB code. The code separates gel and model pixels into one of three groups: gel pixels that do not overlap with the model are shown in green, model pixels not covered by printed gel are highlighted in magenta, and overlapping pixels are shown in white.

Based on the results from acellular prints, agarose-alginate mixtures appeared to be the most promising gel formulation for maintaining print integrity; therefore, only agarose-alginate gel mixtures were used to evaluate cell viability after printing. Chondrocytes were acquired from juvenile bovine stifle joints within 24 hours of death. Articular cartilage was digested overnight with Type 4 collagenase (Worthington, Lakewood, NJ). Approximately 20 M cells/mL were encapsulated within agarose-alginate hydrogels for a final concentration of 3.75% (2.25% agarose + 1.5% alginate) and 5% w/v (3% w/v agarose + 2% w/v alginate) before printing. Constructs were printed as single lines (print width = 0.5 mm, length = 30 mm), cultured for 28 days with chemically-defined media containing growth factors (TGF-β).

On days 0, 7, 14, 21, and 28, samples were stained and imaged to assess cell viability ($n > 5$ per group; Live/Dead kit, Life Technologies, Carlsbad, CA). Images were collected as a z-stack (Swept Field Confocal microscope, Praire Technologies; 10X objective), and a custom written MATLAB algorithm was used to count the number of living (green channel) and dead (red channel) cells. The percentage of living cells was calculated as the number of living cells divided by the total number of cells. Cell viability values greater than 80% were defined as successful.

*Biochemical assay*

Samples were obtained at days 7, 21, and 28 to measure glycosaminoglycan (GAG) composition ($n > 7$ per group). Samples were lyophilized (Labconco, Kansas City, MO) for 48 hours to determine dry weight and digested overnight at 56°C with Protenaise K enzyme (MP Biomedical, Burlingame, CA). GAG content was determined using the colorimetric dimethyl methylene blue (DMMB) assay and normalized by the samples initial wet weight. Data was normalized to the average GAG content at day 7 to assess tissue growth with culture time.

*Statistics*

A one-way analysis of covariance (ANOVA) was performed on the print fidelity parameter, mechanical properties, and cell viability. Significance was assumed at $p < 0.05$. When significance was found, a Bonferroni post-hoc test was performed to compare each agarose or alginate-agarose mixture with the control (Pluronic). Finally, the percentage difference between print parameters for the control and agarose-based gels was calculated.

**Results**

Storage modulus changed slightly with temperature over the range of 25-70 °C (Figure 3A). At physiological temperature of 37°C, 2% agarose had significantly lower storage modulus

values than Pluronic, while there was no significant difference for 3% & 4% agarose or 3.75% and 5% agarose-alginate (Figure 4A). All gels exhibited shear-thinning behavior, with a logarithmically linear decrease in viscosity at higher shear rates (Figure 3B). The shear rate at the wall ($\alpha$) and viscosity ($\beta$) parameters for each gel mixture are presented in Table 1. The magnitude of the slope ($\beta$) was lowest for Pluronic and increased with solid concentration in agarose-only gels, but not agarose-alginate mixtures. The 2% agarose showed significantly lower shear rate and significantly higher viscosity at the extruder wall when compared to Pluronic, and no other gel showed significant differences in either parameter (Figure 3C&D). No clear relationship between viscosity and solid concentration was observed for the range of solid composition evaluated here.

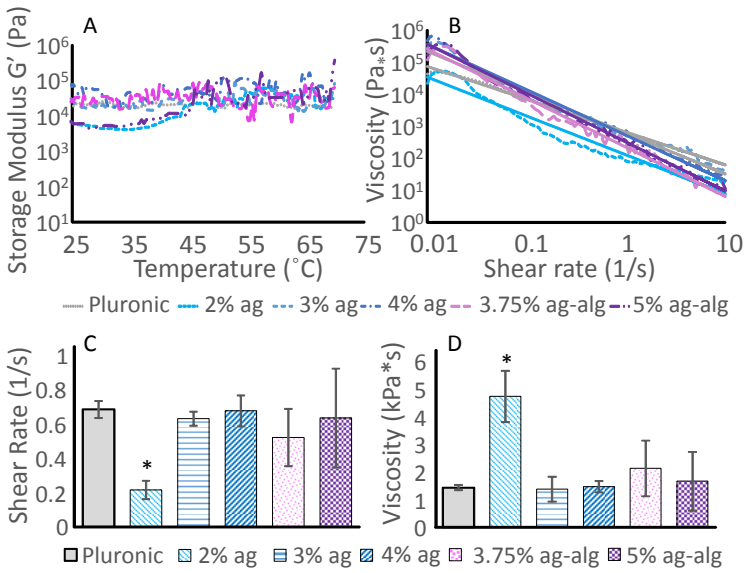


**Figure 3.** Mechanics: A) Storage Modulus vs Temperature, B) Viscosity vs Shear Rate, C) Shear rate felt by gel at extruder wall, and D) Viscosity at extruder wall for all gels. * represents significant difference ($p < 0.05$) to Pluronic.

| Gel | $R^2$ | α | β |
|---|---|---|---|
| **Pluronic** | 0.99 | 654 | -1.0 |
| **2% agarose** | 0.95 | 127 | -1.2 |
| **3% agarose** | 0.97 | 613 | -1.3 |
| **4% agarose** | 0.99 | 522 | -1.4 |
| **3.75% agarose-alginate** | 0.98 | 221 | -1.5 |
| **5% agarose-alginate** | 0.99 | 320 | -1.5 |

**Table 1.** Power fit parameters for viscosity versus shear rate.

The shear yield strength for 3% agarose gels was significantly greater than the shear yield strength of Pluronic (Figure 5B). There were no other significant differences in shear yield strength, but there was high variation in yield strength measured for higher w/v agarose-only gels (3 & 4% agarose). Relaxation experiments showed that recovery after yielding was instantaneous for all gels (Figure 4). Unconfined compression could not be performed on Pluronic because the hydrogel was too soft to test. Agarose gels with 3% w/v and 4% w/v had similar compressive yield strengths, which was greater than 2% w/v agarose and the agarose-alginate mixtures (Figure 4C; $p < 0.001$).

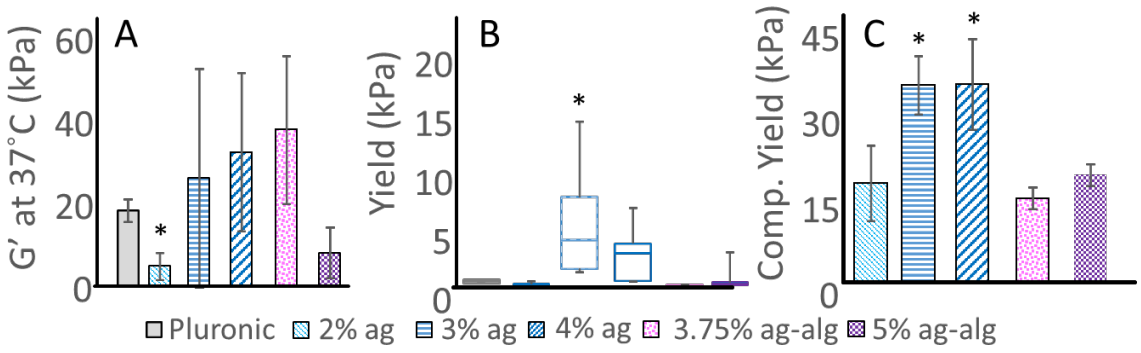

**Figure 4.** Mechanics: A) Storage modulus values at 37°C and B) Shear yield strength for all gels. *represents significant difference ($p < 0.05$) when compared to Pluronic. C) Compressive yield strength for agarose based gels. * represents significant difference ($p < 0.05$) to other groups.

Most gels showed limited shape fidelity, meaning that the construct was not similar to the initial model (Figure 5A-F). Smooth printed lines were achieved with Pluronic, as expected (Figure 5A). However, printability of agarose-based gels varied significantly depending on the agarose concentration and whether it was mixed with alginate (Figure 5B-F). 2% w/v agarose and 3.75% w/v agarose-alginate gels tended to spread beyond the specified print area (Figure 5A & C), while 3% w/v and 4% w/v agarose were too tough to extrude continuously (Figure 5B & D). The calculated print parameter for gels with a greater agarose concentration (*i.e.,* 3 & 4%) were significantly different from the control (Figure 6; $p < 0.001$). Based on the results from printed lines, printing of more complex shapes (*e.g.*, honeycombs) was only attempted with Pluronic and agarose-alginate mixtures (Figure 5G-H).

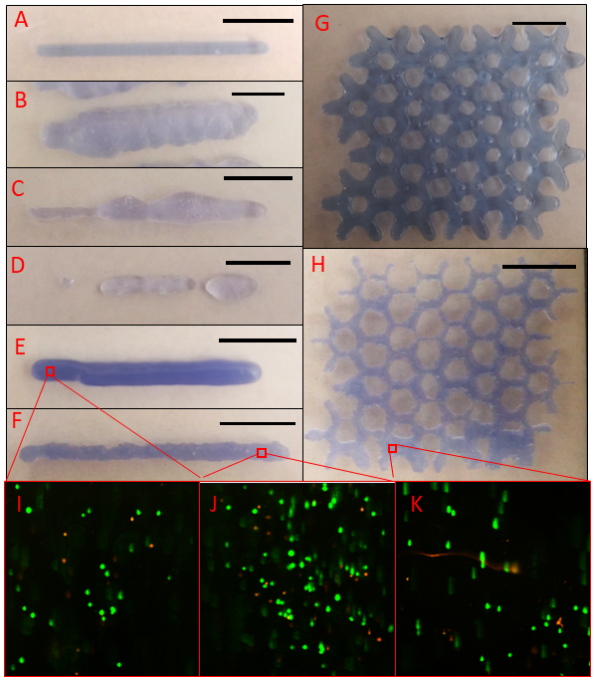

**Figure 5.** 3D printed lines with A) Pluronic, B) 2% agarose, C) 3% agarose, D) 4% agarose, E) 3.75% agarose-alginate, and F) 5% agarose-alginate. Honeycombs printed with G) Pluronic and H) 5% agarose-alginate. Cell viability for I) 3.75% agarose-alginate and J) 5% agarose-alginate printed lines, and from a honeycomb print with K) 5% agarose-alginate at Day 0. Scale bars = 10 mm.

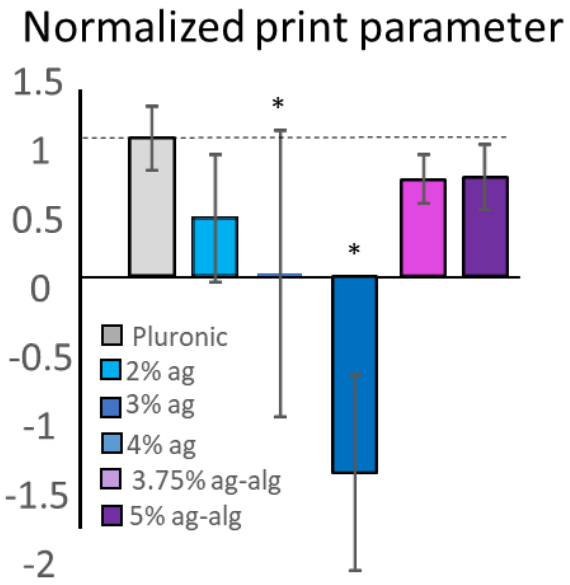


**Figure 6.** Printing parameter results. Numbers above each group represent percentage difference to Pluronic. Groups with an asterisks (*) were significantly different from Pluronic ($p < 0.001$).

Cell viability of agarose-alginate gels fabricated through 3D printing or more established casting techniques showed predominantly living cells throughout the first three weeks of culture (Figure 5I-K, Figure 7A). At day 28, there was a ~20% decrease in cell viability of casted constructs (day 0 = 97.4 ± 0.3%, day 28 = 80.3 ± 14.8%) and a 25% decrease in cell viability of printed constructs (day 0 = 93.3 ± 4.3%, day 28 = 69.6 ± 13.1%; Figure 7). Cell viability of printed constructs was comparable to casted constructs, except that cell viability of printed constructs started to decrease earlier than casted constructs (Figure 7A – day 21). GAG content of all constructs increased with time, with printed constructs containing more than 3 times as much GAG in Day 28 as in Day 7 (Figure 7B).

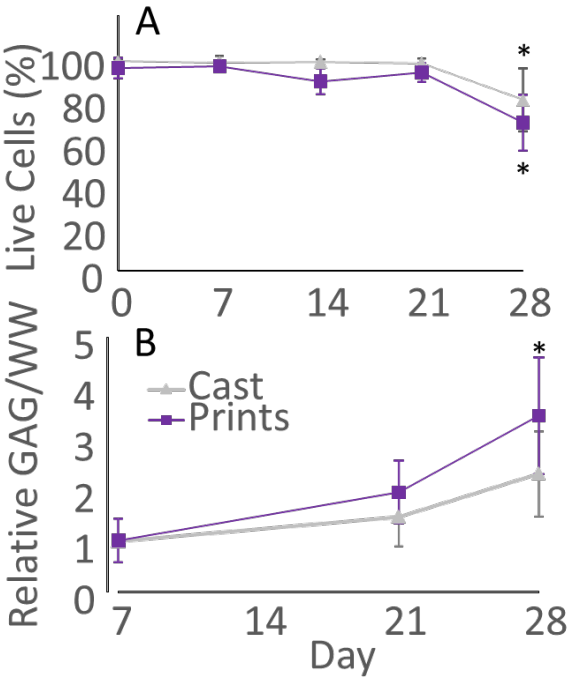


**Figure 7.** A) Cell viability for 5% agarose-alginate (ag-alg) scaffolds. No differences were observed in cell viability between 3D printed lines and traditional casting, except at Day 21 ($p > 0.2$). B) Glycosaminoglycan (GAG) content over sample wet weight (WW) normalized by Day 7 GAG/WW. Error bars represent standard deviation. * represents significant difference to first group.

## Discussion

We evaluated whether hydrogels, that have been successful in developing *de novo* cartilage, have ideal properties as unmodified bioinks for extrusion-based 3D printing. Rheological properties and printability five variations of agarose-based gels were analyzed and compared to Pluronic, a gel with known printing capabilities[8]. Agarose mixed with alginate demonstrated similar shear thinning properties, and yield strength to Pluronic and improved print-shape fidelity when compared to agarose-only gels. Based on print integrity and cell viability results, 5% agarose-alginate mixture was determined to be a suitable material for 3D bioprinting for cartilage tissue engineering. 3D printed agarose-alginate constructs demonstrated excellent cell viability for up to 21 days in culture, as well as improved GAG production.

Many variables factor into print outcomes for extrusion based printing, including print pressure, gel temperature, and gel mechanics. Previous studies have highlighted the importance of extruded materials to have shear thinning properties and a low yield strength. Rheology experiments suggested that 2% agarose, 3.75% agarose-alginate, and 5% agarose could be continuously extruded and therefore printable. All gels exhibited shear thinning behavior defined as a decrease in viscosity when exposed to shear stress (Figure 4). Such behavior has been determined as necessary to extrude from a nozzle and deposit material on a printing bed. However, another requirement that has been previously reported for extrusion is the presence of a shear yield point below 5 kPa. Our results are consistent with these findings, as gels that consistently filled the model area showed yield strengths of that magnitude (Figure 5). Gels that showed limited success with extrusion-based printing had yield strengths significantly higher than Pluronic (3% & 4% agarose; Figures 5 & 7).

To quantify print integrity observations we developed an analysis that resulted in a printing parameter that includes an assessment of the gel's ability to print within the specified print area, accounting for missed areas or overspreading. The addition of a printing parameter suggested that gels that were able to be extruded (2% agarose, 3.75% agarose-alginate, and 5% agarose-alginate) printed with suitable shape fidelity (Figure 7). The print parameter calculated for these gels was not statistically different from Pluronic, nor was it significantly different between gels once normalized by the control (Figure 7). However, it became apparent that 2% agarose and 3.75% agarose-alginate showed significant spreading of gel outside the model area (Figure 6). We initially believed this was due to a delayed recovery of the gel network after extrusion, but rheology experiments showed that all gels maintained an intact network during shearing (Figure 4). Percentage difference between 2% agarose and Pluronic was almost twice as

large as that between agarose-alginate gels and Pluronic (Figure 6). For this reason, 5% agarose-alginate was chosen as the best candidate for cell experiments.

The agarose-alginate mixture (5% w/v) showed excellent cell viability for up to 21 days in culture, as well as production of GAG over a 28 day period in both casted and printed constructs (Figure 8 & 9). Casted constructs have been used extensively in cartilage engineering applications and have been shown to promote matrix production. The absence of significant differences in cell viability between casted constructs and printed constructs agrees with work by Blaeser et al that the printing process does not cause immediate damage to cells. Printed constructs also showed a slightly higher GAG content than casted constructs, although there was no significant difference when compared to printed constructs (Figure 9; p-value). We believe that this difference was influenced by geometric reasons, as printed lines are thinner (~0.5mm wide) than casted constructs (diameter = 2.27 mm) and as such there is less distance for nutrients in the media to travel. The similarities in GAG production between casts and prints lead us to believe that the 5% w/v agarose-alginate gel is a suitable bioink.

Rheological properties for all gels were evaluated at physiological temperature (37°C) instead of a wider range to match the temperature during cell-based printing.. Given that agarose is a thermoset material, it remains plausible that agarose-only gels can produce constructs with high shape fidelity under different temperature conditions. The findings in this study did not show a definitive rheological property that correlated to print integrity, but our results are consistent with previous findings that suggest yield strength and shear-thinning are factors in being able to extrude a material continuously (Figure 4 & 5). The primary focus of cell-based test in this study was to evaluate cell viability. Future work will evaluate matrix production of other constituents, such as collagen, and evaluate tissue mechanics over time.

## Conclusions

In conclusion, the 5% w/v agarose-alginate mixture was ideal for extrusion-based bioprinting of 3D cartilage constructs. The mixture was able to print high shape fidelity structures comparable to Pluronic without the necessity of additional crosslinking or printing inside sacrificial materials, a technique that may affect long-term performance by including additional steps in the fabrication process. Moreover, the agarose-alginate mixture maintained excellent cell viability and supported GAG production. Therefore, extrusion-based printing may provide researchers with an easy-to-manufacture technique for developing complex engineered tissues.

**Acknowledgements**

This material is based upon work supported by the National Science Foundation Graduate Research Fellowship Program under Grant No. (DGE 1106400) and the National Academy of Engineers (Grainger Foundation). Any opinions, findings, and conclusions or recommendations expressed in this material are those of the authors and do not necessarily reflect the views of the National Science Foundation. We would like to also thank Dr. Kevin Healy (UC Berkeley) for allowing use of his rheometer for this study.

**Competing interests statement**

The authors have no competing interests to declare.

## References


1. Ostendorf, R.H., et al., *Cyclic loading is harmful to articular cartilage from which proteoglycans have been partially depleted by retinoic acid.* Osteoarthritis Cartilage, 1995. **3**(4): p. 275-84.
2. Boschetti, F., et al., *Biomechanical properties of human articular cartilage under compressive loads.* Biorheology, 2004. **41**(3-4): p. 159-66.
3. Pal, S., *Design of Artificial Human Joints and Organs*. 1 ed. Vol. 1. 2014: Springer US. 419.
4. Fang, L., Y. Leng, and P. Gao, *Processing and mechanical properties of HA/UHMWPE nanocomposites.* Biomaterials, 2006. **27**(20): p. 3701-7.
5. Goodman, S., et al., *Tissue ingrowth and differentiation in the bone-harvest chamber in the presence of cobalt-chromium-alloy and high-density-polyethylene particles.* Journal of Bone & Joint Surgery, 1995. **July** (American).
6. Ford, A.C., et al., *A Modular Approach to Creating Large Engineered Cartilage Surfaces.* J Biomech, 2017. **In Press**.
7. Nicodemus, G.D. and S.J. Bryant, *Cell encapsulation in biodegradable hydrogels for tissue engineering applications.* Tissue Eng Part B Rev, 2008. **14**(2): p. 149-65.
8. Muller, M., et al., *Nanostructured Pluronic hydrogels as bioinks for 3D bioprinting.* Biofabrication, 2015. **7**(3): p. 035006.
9. O'Connell, G.D., et al., *Toward Engineering a Biological Joint Replacement.* The journal of knee surgery, 2012. **25**(3): p. 187-196.
10. Jeong, J.H., et al., *Human Cartilage Tissue Engineering with Pluronic and Cultured Chondrocyte Sheet.* Key Engineering Materials, 2007. **342-343**: p. 89-92.
11. O'Connell, G.D., J.K. Leach, and E.O. Klineberg, *Tissue Engineering a Biological Repair Strategy for Lumbar Disc Herniation.* Biores Open Access, 2015. **4**(1): p. 431-45.
12. Ford, A.C., et al., *Modular Tissue Engineered Cartilage Surfaces*, in *Summer Biomechanics Bioengineering and Biotransport Conference (SB3C)*. 2015: Utah, USA. p. 2.
13. Pluen, A., et al., *Diffusion of macromolecules in agarose gels: comparison of linear and globular configurations.* Biophys J, 1999. **77**(1): p. 542-52.
14. Bian, W., et al., *Mesoscopic hydrogel molding to control the 3D geometry of bioartificial muscle tissues.* Nature protocols, 2009. **4**(10): p. 1522-1534.
15. Tan, A.R. and C.T. Hung, *Concise Review: Mesenchymal Stem Cells for Functional Cartilage Tissue Engineering: Taking Cues from Chondrocyte-Based Constructs.* Stem Cells Transl Med, 2017. **6**(4): p. 1295-1303.
16. O'Connell, G., J. Garcia, and J. Amir, *3D Bioprinting: New Directions in Articular Cartilage Tissue Engineering.* ACS Biomaterials Science & Engineering, 2017.
17. Stanton, M.M., J. Samitier, and S. Sanchez, *Bioprinting of 3D hydrogels.* Lab Chip, 2015. **15**(15): p. 3111-5.
18. Wei, J., et al., *3D printing of an extremely tough hydrogel.* RSC Adv., 2015. **5**(99): p. 81324-81329.
19. Adamkiewicz, M. and B. Rubinsky, *Cryogenic 3D printing for tissue engineering.* Cryobiology, 2015. **71**(3): p. 518-21.

20. Mouser, V.H., et al., *Yield stress determines bioprintability of hydrogels based on gelatin-methacryloyl and gellan gum for cartilage bioprinting.* Biofabrication, 2016. **8**(3): p. 035003.
21. Huang, Y., et al., *3D bioprinting and the current applications in tissue engineering.* Biotechnol J, 2017. **12**(8).
22. Augst, A.D., H.J. Kong, and D.J. Mooney, *Alginate hydrogels as biomaterials.* Macromol Biosci, 2006. **6**(8): p. 623-33.
23. DeKosky, B.J., et al., *Hierarchically designed agarose and poly(ethylene glycol) interpenetrating network hydrogels for cartilage tissue engineering.* Tissue Eng Part C Methods, 2010. **16**(6): p. 1533-42.
24. Duan, B., et al., *3D bioprinting of heterogeneous aortic valve conduits with alginate/gelatin hydrogels.* J Biomed Mater Res A, 2013. **101**(5): p. 1255-64.
25. J., P. and C.-W. Wang, *An Investigation on the Influence of Pore Size and Porosity of Sponge on Maximum Cell Concentration.* 2010: p. 1-9.
26. Kuo, C.K. and P.X. Ma, *Ionically crosslinked alginate hydrogels as scaffolds for tissue engineering: part 1. Structure, gelation rate and mechanical properties.* Biomaterials, 2001. **22**(6): p. 511-21.
27. Lee, K.Y. and D.J. Mooney, *Alginate: properties and biomedical applications.* Prog Polym Sci, 2012. **37**(1): p. 106-126.
28. Muller, M., et al., *Alginate Sulfate-Nanocellulose Bioinks for Cartilage Bioprinting Applications.* Ann Biomed Eng, 2017. **45**(1): p. 210-223.
29. Ozbolat, I.T., K.K. Moncal, and H. Gudapati, *Evaluation of bioprinter technologies.* Additive Manufacturing, 2017. **13**: p. 179-200.
30. Diniz, I.M., et al., *Pluronic F-127 hydrogel as a promising scaffold for encapsulation of dental-derived mesenchymal stem cells.* J Mater Sci Mater Med, 2015. **26**(3): p. 153.
31. Gioffredi, E., et al., *Pluronic F127 Hydrogel Characterization and Biofabrication in Cellularized Constructs for Tissue Engineering Applications.* Procedia CIRP, 2016. **49**: p. 125-132.
32. Ozbolat, I.T. and M. Hospodiuk, *Current advances and future perspectives in extrusion-based bioprinting.* Biomaterials, 2016. **76**: p. 321-43.
33. Baird, D.G. and D.I. Collias, *Polymer processing: principles and design*. 2014: John Wiley & Sons.
34. Smith, P.T., et al., *Chemical modification and printability of shear-thinning hydrogel inks for direct-write 3D printing.* Polymer, 2018.
35. Guvendiren, M., et al., *Designing Biomaterials for 3D Printing.* ACS Biomaterials Science & Engineering, 2016. **2**(3D Bioprinting): p. 1679-1693.
36. Wu, Z., et al., *Bioprinting three-dimensional cell-laden tissue constructs with controllable degradation.* Sci Rep, 2016. **6**: p. 24474.
37. Wang, L., et al., *Evaluation of sodium alginate for bone marrow cell tissue engineering.* Biomaterials, 2003. **24**(20): p. 3475-81.
38. Mauck, R.L., et al., *Functional Tissue Engineering of Articular Cartilage Through Dynamic Loading of Chondrocyte-Seeded Agarose Gels.* Journal of Biomechanical Engineering, 2000. **122**: p. 252-260.

36. Smith, P. et al. *Chemical modification and printability of shear thinning hydrogels for direct-write 3D printing.* Polymer, 2018.

**For Table of Contents Only:**

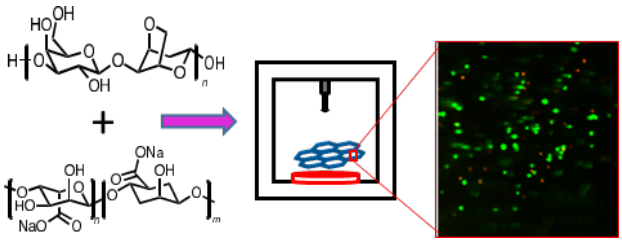

TOC Graphic: Agarose-alginate bioinks